

ORIGINAL ARTICLE

# Novel Ti surface coated with PVA hydrogel and chitosan nanoparticles with antibacterial drug release: An experimental in vitro study

Pablo Yael Carrazco Ávila<sup>1</sup>  | Teresa Arias Moliz<sup>2</sup> | Juan Ignacio Rosales Leal<sup>1</sup>  | Pilar Baca<sup>1</sup> | Miguel Ángel Rodríguez Valverde<sup>3</sup> | María Encarnación Morales Hernandez<sup>4</sup>

<sup>1</sup>Department of Stomatology, School of Dentistry, Campus de Cartuja s/n, University of Granada, Granada, Spain

<sup>2</sup>Department of Microbiology, School of Dentistry, University of Granada, Granada, Spain

<sup>3</sup>Department of applied Physics, School of Science, University of Granada, Granada, Spain

<sup>4</sup>Department of Pharmacy and Pharmaceutical Technology, School of Pharmacy, Campus de Cartuja s.n., University of Granada, Granada, Spain

## Correspondence

Juan Ignacio Rosales Leal, Department of Stomatology, School of Dentistry, Campus de Cartuja s/n, University of Granada, Granada 18071, Spain.  
Email: [irosales@ugr.es](mailto:irosales@ugr.es)

## Abstract

**Objectives:** The aims of this study were to design a novel titanium surface coated with a PVA hydrogel matrix and chitosan-based nanoparticles and to investigate the antibiotic release and its ability to inhibit microbial activity.

**Methods:** Two drug delivery systems were developed and mixed. Chitosan-based nanoparticles (NP) and a polyvinyl alcohol film (PVA). The size,  $\zeta$ -potential, stability, adhesive properties, and encapsulation profile of NP, as well as the release kinetics of drug delivery systems and their antimicrobial ability of PVA and PVANP films, were studied on Ti surfaces. The systems were loaded with doxycycline, vancomycin, and doxepin hydrochloride.

**Results:** Nanoparticles presented a  $\zeta$ -potential greater than 30 mV for 45 days and the efficiency drug encapsulation was  $26.88\% \pm 1.51\%$  for doxycycline,  $16.09\% \pm 10.24\%$  for vancomycin and  $17.57\% \pm 11.08\%$  for doxepin. In addition, PVA films were loaded with 125  $\mu\text{g/mL}$  of doxycycline, 125  $\mu\text{g/mL}$  of vancomycin, and 100  $\mu\text{g/mL}$  of doxepin. PVANP-doxycycline achieved the antibacterial effect at 4 h while PVA-doxycycline maintained its effect at 24 h.

## KEYWORDS

biofilm, chitosan, dental implant, dental plaque, doxepin hydrochloride, doxycycline, drug delivery system, nanoparticles, polyvinyl alcohol, vancomycin

**Abbreviations:** ATP, adenosine triphosphate; CFU, colony-forming units; Cs, chitosan; DDs, drug delivery systems; NP, nanoparticles; PVA, polyvinyl alcohol; RLU, relative light units.

This is an open access article under the terms of the [Creative Commons Attribution-NonCommercial-NoDerivs](https://creativecommons.org/licenses/by-nc-nd/4.0/) License, which permits use and distribution in any medium, provided the original work is properly cited, the use is non-commercial and no modifications or adaptations are made.

© 2024 The Authors. *Clinical Implant Dentistry and Related Research* published by Wiley Periodicals LLC.

## Summary Box

### What is known

Polymer-based matrices have been used as a vehicle to transport active principles, allowing targeted delivery of the drug. Polyvinyl alcohol and chitosan have been used to design gel systems, membranes, scaffolds, and nanoparticles, with the intention of avoiding side effects caused by systemic administration.

### What this study adds

- This study designed two drug delivery systems that were combined to provide targeted delivery with the intention of modifying the surface of dental implants, providing a bacteriostatic, osteoinductive, and therapeutic effect.
- Ti surfaces were successfully covered with a drug delivery system based on polyvinyl alcohol films and chitosan nanoparticles.
- Polyvinyl alcohol and chitosan nanoparticles on Ti are loadable with antibacterial drugs.
- Although vancomycin and doxepin showed antibacterial effect, doxycycline induced the greatest inhibition of bacterial activity and growth for the longest time.
- Bacterial adhesion was conditioned by drug release and not by surface characteristics (topography or wetting).

## 1 | INTRODUCTION

Osseointegration (Oss) refers to the process by which a dental or orthopedic implant forms a direct functional connection with the surrounding bone tissue, without intervening soft tissue.<sup>1</sup> Oss involves the formation of new bone tissue around the implant, which eventually anchors it firmly in place. The speed and quality of the cellular response will ensure a correct osseointegration and supply the stability and support for the implant device. It will allow complex interventions such as post-extraction implants, immediate loading, or combination with bone regeneration.<sup>2,3</sup> Therefore, implant design, surgical technique, surface quality, and bone condition are crucial for bone wound healing. Despite this, there are some unsuccessful treatments due to a variety of reasons such as infection, inflammation, or some systemic diseases, that lead to damage to the human cellular response.<sup>4,5</sup>

Titanium and titanium alloys are widely used in dental implants. Both are vulnerable to infection, due to biofilm formation on the surface and compromised immune capacity at the implant/tissue interface.<sup>6,7</sup> That is why it is extremely important to maintain bone tissue in an aseptic environment during and after implantation. This moment is the riskiest time for infection because the local defense mechanism is seriously disrupted by surgical injuries.<sup>7</sup> In fact, the most frequent cause of early implant failure is infection following bacterial contamination of the surgical site.<sup>8</sup>

Focusing on avoiding and controlling bacterial adhesion, there are different approaches to develop a Ti surface that delivers drugs exerting antimicrobial activity.<sup>9,10</sup> One of the common drug delivery systems (DDs) to prevent infections is the use of coated titanium implant. DDs on titanium implants have been loaded with different antibiotics for antimicrobial purposes, including gentamicin,

vancomycin, doxycycline, and other similar drugs.<sup>7,10-13</sup> These systems have shown stability and predictability and are applied locally reducing the side effects.<sup>8,14-16</sup> DDs can be prepared using one or multiple techniques such as films, nanoparticles (NPs), hydrogels, scaffolds, and titania nanotubes.<sup>8-10</sup> The use of synthetic and natural polymers such as polyvinyl alcohol (PVA) and chitosan (Cs) to create a three-dimensional matrix able to carry drug has been widely studied.<sup>14,17-19</sup> PVA is a synthetic water-soluble polymer and has gained significant attention in the pharmaceutical industry due to its biocompatibility, low toxicity, and ability to form films.<sup>19,20</sup> Because of its adhesive formulations, film containing cross-linked PVA has a lower erosion rate, resulting in controlled drug release.<sup>21</sup> In addition, PVA has been used for oral, ocular, and gastrointestinal drug delivery.<sup>22</sup>

Another option is the use of natural polymer as chitosan. Due to its versatility, chitosan has attracted great interest and it has also been used to develop NPs.<sup>23,24</sup> Cs results from the deacetylation of chitin and exhibits interesting physicochemical and biological properties.<sup>25-28</sup> Although Cs is insoluble in water, it can be dissolved in acidic environments. It shows biocompatibility and biodegradability with low toxicity, making it suitable for various biomedical applications.<sup>29,30</sup> In addition, chitosan possesses a bioadhesive surface and bacteriostatic properties.<sup>13,31</sup>

PVA have been used for dermal or mucosal patches because of their ease of manufacture and their effectiveness in carrying drugs and covered NPs.<sup>20,21,32,33</sup> PVA has been study to formulate films that provide a solubilizing environment to incorporate hydrophilic drugs such as chlorhexidine and doxycycline.<sup>17</sup> The use of drug-loaded NPs has also been introduced in the design of implant surfaces.<sup>16,17</sup> This reduces the solubility and dispersion of the drug and makes it more available in the medium where it is released.<sup>13</sup> NP immobilization is achieved by depositing them on nanotubes using cathodic

electrodeposition or by spray coating and drop casting.<sup>16,17,34</sup> Both polymers, PVA and Cs have been used simultaneously to create a film to facilitate the targeted release of curcumin-based NPs, as well as have been loaded with benzalkonium bromide.<sup>20,33</sup> Nevertheless, to our knowledge, these NPs have not been included in PVA films for titanium surface coating. It is necessary to continue developing methods to coat surfaces for bone implants with this type of films and to understand its biological effect. The development of coatings with PVA and drug-loaded NPs may contribute to reducing the risk of surgical site infections as well as accelerating bone response.

The present article focuses on developing a polyvinyl alcohol hydrogel matrix that can effectively transport NPs and be loaded with various drugs. This innovative DDs could improve the bioactivity and biocompatibility of therapeutic agents, as well as prolong their time of action. Furthermore, the carrying systems can liberate antimicrobial drugs and prevent the early bacteria colonization and immediate surgical site infection. The aim of this study was to design and develop a new titanium surface coated with a PVA hydrogel matrix and chitosan-based NPs to evaluate drug release and its antimicrobial potential.

## 2 | MATERIALS AND METHODS

### 2.1 | Study design

DDs were incorporated into Ti surfaces using chitosan NPs and a polyvinyl alcohol film to transport doxycycline, vancomycin, and doxepin hydrochloride. The impact of DDs on bacterial activity was analyzed. The study analyzed the size,  $\zeta$ -potential, and encapsulation profile of NPs and evaluated the release kinetics of DDs. Microbial viability and activity were assessed using colony forming units (CFU) count, the adenosine triphosphate (ATP) assay, and flow cytometry test by using the live/dead technique. The antibiotic efficacy of the systems in preventing the formation of biofilm over time was evaluated using confocal laser scanning microscopy (CLSM). The development and study groups are shown in Figure 1.

### 2.2 | Surface preparation

Cylinders of commercially pure ASTM grade II Ti (Manfredi, S. Secondo di Pinerolo, Italy) were used. The samples were cut into small disks measuring 15 mm in diameter and 2 mm in thickness. Subsequently, the disks were cleaned by immersing them in 99.5% acetone and subjected to ultrasound using deionized water at 36°C for 10 min. The samples were then polished using a metallographic polishing protocol that involved using silicon carbide papers ranging from no 500, 800, 1200, 2500, and 4000 grit.<sup>35</sup> To control the polishing process, all specimens were observed under optical stereomicroscope (Olympus SZ-PT, Tokyo, Japan) at 100 $\times$  after each step. The cleaning protocol was repeated between each silicon carbide paper to remove titanium shavings deposited on the surface of the disks.

Finally, samples were treated with radio frequency plasma of argon (Emitech, KX1050 Plasma Asher) to a power of 25 W at 200°C for 15 min to remove organic impurities. Immediately after plasma treatment, the oxidation state of the samples was stabilized in water for 24 h. The samples were allowed to dry for 24 h at 37°C.<sup>36</sup>

### 2.3 | Design and development of drug delivery systems

Three different approaches were used for targeted drug delivery: directly on the polished Ti surface, via a polyvinyl alcohol biofilm, and through a polyvinyl alcohol biofilm loaded with chitosan NPs.

#### 2.3.1 | Drug analytical method

Three different drugs were used: doxycycline (Panreac AppliChem, Barcelona, Spain), vancomycin (Pfizer, Madrid, Spain), and doxepin hydrochloride (Fagron, Barcelona, Spain). First, it was necessary to study the calibration curve of drugs. Different concentrations were analyzed following Beer–Lambert's law to figure out drug concentrations. Doxycycline (250  $\mu\text{g/mL}$ ), vancomycin (250  $\mu\text{g/mL}$ ), and doxepin hydrochloride (100  $\mu\text{g/mL}$ ) concentrations were selected and measured by UV-spectrophotometry at 270 nm, 280 nm, and 292 nm ( $\lambda_{\text{max}}$ ), respectively. The method was previously validated and verified for accuracy, precision, and linearity. A Perkin-Elmer UV–Vis Lambda 40 UV-spectrophotometer was used to take all measurements.

#### 2.3.2 | Surface drug loading

##### *Synthesis of chitosan nanoparticles*

For this study, the chitosan NPs were synthesized using the ionic gelation technique.<sup>37–39</sup> The procedure involved dispersing 0.069% w/v of low molecular weight chitosan (Sigma Aldrich, Madrid, Spain) in deionized water, followed by the addition of 1% v/v acetic acid to the Cs solution ( $\text{C}_6\text{H}_{11}\text{NO}_4$ )<sub>n</sub>. The resulting solution was stirred at room temperature for 15 min. A solution of sodium tripolyphosphate (TPP) with a concentration of 0.2% w/v (Alfa Aesar, Kandel, Germany) was prepared by dissolving it in deionized water. The pH of the TPP solution was then adjusted to 5 by adding 0.1 M HCl (37%) (VWR International, Fontenay-sous-Bois, France).

To synthesize NP, the chitosan solution was combined with the TPP solution by slowly adding 645  $\mu\text{L}$  of the TPP solution and stirring the mixture for 4 h at room temperature until the final volume of 9 mL was achieved. The Cs:TPP ratio used in the synthesis was 9:1.<sup>23,38</sup> The size, polydispersity index (PDI), and  $\zeta$ -potential of the NPs were analyzed using the dynamic light scattering method. Measurements were made at  $25.0 \pm 0.5^\circ\text{C}$  using a Malvern Zetasizer Nano ZS<sup>®</sup> (Malvern Instruments Ltd., Malvern, UK) and were performed in triplicate. The hydrodynamic diameter was expressed in nanometers and the  $\zeta$ -potential was reported in millivolts (mV).

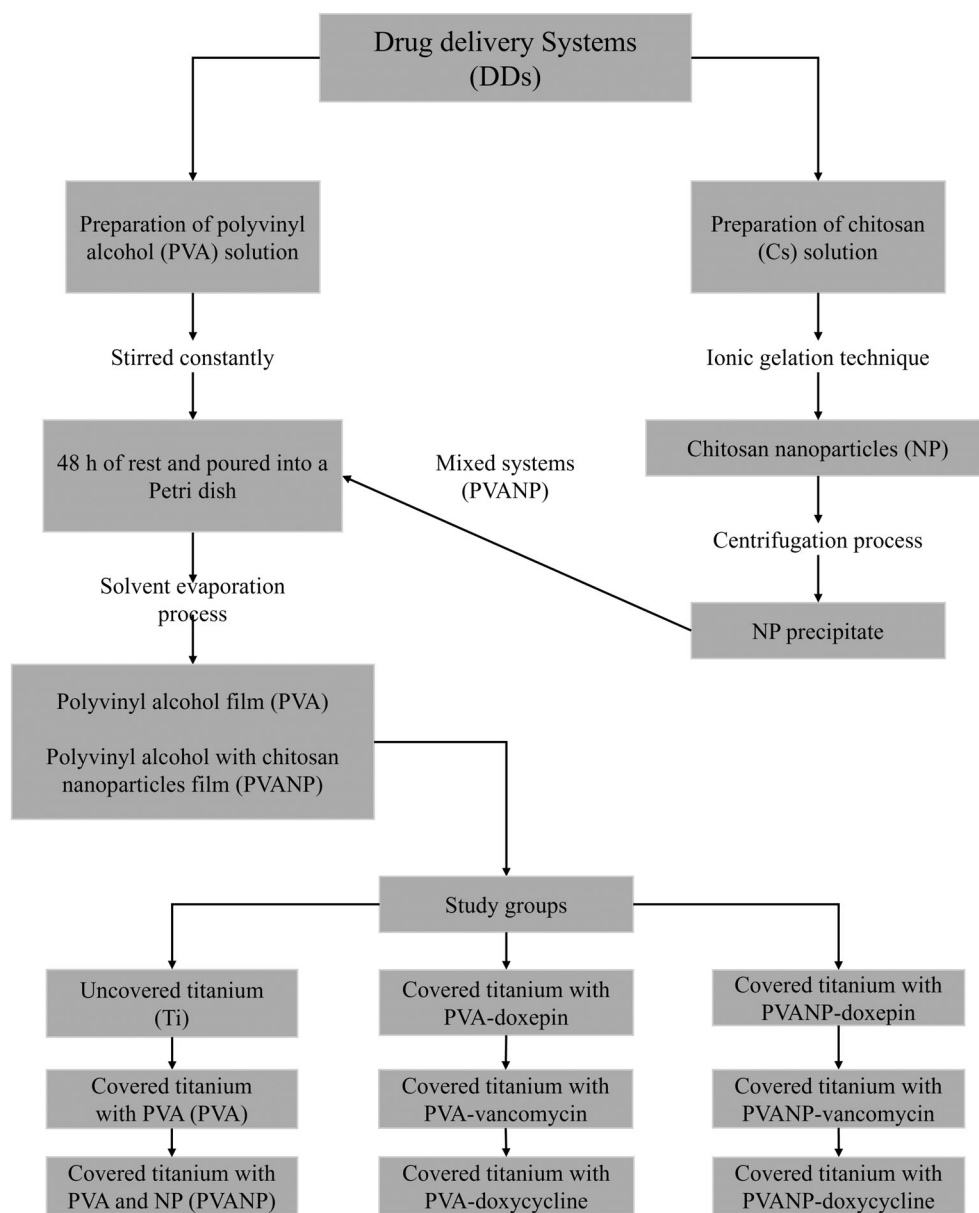


**FIGURE 1** Illustrative representation of the development and study groups of drug delivery systems.

#### Drug encapsulation efficacy DEE%

In the same way, the drug encapsulation efficiency (DEE%) was evaluated. NP dispersions were subjected to centrifugation at 14 000 rpm for 20 min to obtain a solid precipitate to determine drug encapsulation efficacy. The NP was redispersed in 4.5 mL of deionized water to achieve a higher volume concentration. The supernatants were analyzed using UV spectrophotometry following the same process mentioned earlier, and the DEE% was calculated using the given formula:

$$\text{DEE\%} = \frac{\text{weight of drug in nanoparticles}}{\text{weight of initially used drug}} \times 100.$$

#### Adhesive properties

On the other hand, it is important to know the adhesive properties of NP. A mucin solution ( $0.5 \text{ mg mL}^{-1}$ ) was added to PBS at pH 6, and then

the NPs were combined with the mucin solution at a 1:1 (v/v) ratio and incubated at  $37^\circ\text{C}$  with constant stirring. After 1, 2, 3, and 4 h, 1 mL of the NP and mucin mixture was extracted, and the supernatant was evaluated using the spectrophotometric method at 255 nm.<sup>40</sup> The following formula was used to compute the adhesion of mucin to the NPs:

$$\text{Mucin binding efficiency (\%)} = \frac{\text{Initial mucin (amount)} - \text{free mucin (amount)}}{\text{Initial mucin (amount)}} \times 100.$$

The adhesive effects of drug-loaded and free-drug chitosan were calculated by measuring the zeta potential. (Malvern Zetasizer Nano ZS®, Malvern, UK).

#### Polyvinyl alcohol biofilm and mixed system

It was used as a purified PVA powder (molecular formula:  $(\text{C}_2\text{H}_4\text{O})_n$ ;  $M = 72\,000 \text{ g/mol}$ ). The biofilms were elaborated using the solvent

evaporation process, as described by previous studies.<sup>14,21</sup> In the first step, Polyvinyl alcohol (Panreac, Barcelona, Spain) with a concentration of 3% w/v was prepared. The PVA powder was dispersed in deionized water and stirred constantly at room temperature until it was completely dissolved. The solutions were left undisturbed for 48 h to remove any trapped air bubbles. Subsequently, 4.5 mL of the PVA solution was poured into a Petri dish and allowed to dry at 37°C for 24 h. The PVA biofilms obtained showed a uniform and smooth surface with no visible air bubbles. The solubility of the PVA was counted and total films was dissolved after 60 min of immersion.<sup>41</sup> To incorporate drugs into the biofilms, PVA powder was poured into solutions with the drug concentrations mentioned above. Finally, a mixed system was also designed in which the polyvinyl alcohol biofilm functioned as a matrix to transport the NPs. To achieve this, unloaded biofilms were prepared as described earlier. The NPs were centrifuged at 14 000 rpm for 20 min, followed by removal of the supernatant. The resulting precipitate was then redispersed in 4.5 mL of PVA solution. The samples were allowed to dry for 48 h. The solubility of the PVANP was counted and total films was dissolved after 90 min of immersion.<sup>41</sup>

## 2.4 | Surface characterization

### 2.4.1 | Topography and wetting

The topographies were obtained using a white light confocal microscope (PLμ Sensofar-Tech, Barcelona, Spain). Three disks per group were examined and three topographies were acquired using an EPI ×50 objective, with a scan size area of 285 × 209 μm<sup>2</sup>. The topographic parameters were obtained using microscope software and included average roughness ( $R_a$ ), peak roughness ( $R_p$ , maximum relative height), valley roughness ( $R_v$ , maximum relative depth), absolute height ( $R_{max/t} = R_p + R_v$ ), root mean square ( $R_q$ ), skewness ( $R_{sk}$ ), and kurtosis ( $R_{ku}$ ).<sup>35</sup> Topographic analyses were used to control the polishing procedure.

### 2.4.2 | Wettability test

Wettability was measured through the contact angle of spreading water sessile drops. MilliQ water drops (1 μL of volume) were dispensed using a micropipette (Eppendorf, Hamburg, Germany) at 25°C. Three specimens were analyzed per group and three drops were deposited on each surface. Once the drop was dispensed on the substrate, top-view images of drop were acquired and analyzed by Axisymmetric Drop Shape Analysis. Contact angles were directly computed by ad-hoc designed software.<sup>42</sup>

### 2.4.3 | Scanning electron microscopy (SEM)

The DDs were analyzed for size, shape, and surface properties using SEM (Hitachi S-5-10, Tokyo, Japan). Before examination, the samples

were mounted on an aluminum stub using a double-sided adhesive tape and making it electrically conductive by coating it with a thin layer of gold (approximately 20 nm) in vacuum.<sup>14</sup>

## 2.5 | In vitro drug release assay

The release profile of the polyvinyl alcohol and polyvinyl alcohol with NPs films were immersed carefully in 50 mL of artificial saliva in beakers and placed in a hot bath. The solutions were shaken at 300 rpm for 6 h at 37 ± 0.5°C. With the same procedure as above, at the previously established times, 1 mL was removed to determine drug release, and the solution was refreshed with 1 mL of artificial saliva at each pipetting.

## 2.6 | Antimicrobial activity

### 2.6.1 | Microbial sample collection

The study protocol was approved by the Ethics Committee of the Institution where the research was conducted no. 2708/CEIH/2022. All participants supplied informed consent prior to the study. Clinical microbial samples of supragingival dental plaque were taken from 15 patients who attended the University clinic for dental scaling. Microbial samples were included in tubes with Tryptic enriched Soy Broth solution (TSB) and stored at −20°C for further analysis.

### 2.6.2 | Multi-species biofilm formation on titanium disks and antimicrobial analysis

Bacterial suspensions were prepared in TSB and adjusted to a concentration of 10<sup>8</sup> CFU/mL. Natural multispecies biofilms were cultured on the surface of the disks. For this purpose, sterile titanium disks with different surface treatments were transferred to the wells a 12-well plate (JET Biofil, Guangzhou, China) inoculated with 1 mL of the bacterial suspension. The biofilms were allowed to grow for 4 and 24 h at 37°C under anaerobic conditions. At 4 and 24 h, the disks were washed with 2 mL of saline solution to remove loosely adhered bacteria to the biofilm. The disks were thereafter transferred into tubes containing 1 mL of TSB, vortexed for 10 s, and sonicated for 10 min in an ultrasonic bath to recover the bacteria in the culture media. A total of 15 samples per group and incubation time were evaluated. The assessment of antimicrobial activity was conducted by two different methods:

**Colony-forming units (CFUs):** The recovered biofilm was serially diluted (10<sup>−1</sup> – 10<sup>−5</sup>) and 10 μL aliquots of each dilution were seeded in blood agar medium. Plates were incubated under anaerobic conditions for 72 h at 37°C. After this period, colonies were counted, and the number of CFU/mL was calculated. The results were expressed as the Log<sub>10</sub>(CFUs).

**ATP assay:** 100 μL of the recovered bacterial suspension was added to 100 μL of BacTiter-Glow reagent (Promega, Madison, WI) in

a black 96-well plate and incubated for 5 min. The luminescence produced was measured with a luminometer (GloMax; Promega, Madison, WI). The mean of the signals from the bacterial culture minus the mean of the enriched TSB alone (blank) was calculated and expressed as relative light units (RLUs).<sup>43</sup>

Three additional samples per group were contaminated as explained above and prepared for CLSM observation. For this purpose, after incubation, the samples were rinsed with saline solution and were stained the LIVE/DEAD BacLight Bacterial Viability kit (Invitrogen, Eugene, OR).<sup>44</sup> This kit contains Syto 9 which binds to bacteria with intact membranes and propidium iodide (PI) which labels membrane damaged bacteria. The disks were stained with the dyes for 15 min and were thereafter observed under a CLSM (Leica TCS-SP5 II, Leica Microsystems, Mannheim, Germany). The excitation/emission wavelengths were 494/518 nm for Syto-9 and 536/617 nm for PI. A total of 10 microscopic confocal volumes (stacks) from random areas were obtained from each group using a 40X oil lens with a 1-mm step size and a resolution of  $512 \times 512$  pixels. Each picture represented an area of  $837 \times 837 \mu\text{m}$ .

For quantification purposes, bioimage\_L software ([http://www.bioimageL.com/get\\_bioimage\\_L](http://www.bioimageL.com/get_bioimage_L)) was used.<sup>45</sup> The variable evaluated in each group was the biovolume of membrane-intact cells.

After incubation period, three samples per group were treated with 2.5% glutaraldehyde in PBS (pH 7.2) for 20 min to fix the bacteria, followed by dehydration in graded alcohols, critical point dried and carbon coated. Finally, the surface was examined under scanning electron microscope (Leo 1430-VP, Carl Zeiss, Oberkochen, Germany).

## 2.7 | Statistical analysis

Size,  $\zeta$ -potential, and PDI were analyzed using Fisher's test, followed by the *t*-student test. Contact angle and roughness parameters were analyzed by analysis of variance and a student-Newman Keuls multiple comparison test. All data were expressed as the mean  $\pm$  standard deviation and the results were observed as a significant difference when  $p < 0.05$ . For the antimicrobial assays, the Shapiro-Wilk test was used to check the normality of the transformed variables. After confirming that did not follow a normal distribution, multiple comparisons were performed by means of the Kruskal-Wallis test, and pair-by-pair comparisons between groups and between times of incubation (4 vs. 24 h), by Mann-Whitney test. The level of significance was set at  $p < 0.05$ . Statistical analyses were performed using SPSS 20.0 software.

## 3 | RESULTS

### 3.1 | Physicochemical characterization of the nanoparticles

Based on the results presented in Table 1, a decrease in hydrodynamic diameter of 20.27 nm was observed for NP-doxepin and 5.09 nm for NP-vancomycin. Statistically, the size reduction did not present a

significant difference ( $p > 0.05$ ). An increase of 226.93% was detected for NP-doxycycline. In addition, another essential parameter used to define particle size uniformity is PDI. Similarly, as hydrodynamic diameter, PDI of NP-doxepin and NP-vancomycin did not show a statistically significant difference, but NP-doxycycline anew showed the highest parameter. NP-doxycycline showed a statistically significant difference in both cases ( $p < 0.05$ ).

The  $\zeta$ -potential shown in Table 1 was similar for all the groups except for NP-vancomycin which obtained highest value ( $p < 0.05$ ). Contrary to the size and PDI parameters, where NP-doxycycline presented the highest values, NP-vancomycin showed an increase of 3.78 mV in their surface charge, showing a statistically significant difference ( $p < 0.05$ ). On the other hand, the  $\zeta$ -potential as a function of time was stable. Measurements were taken every 15 days for 45 days and NPs were stable over time.

The drug encapsulation efficiency values obtained were  $26.88\% \pm 1.51\%$  for doxycycline,  $16.09\% \pm 10.24\%$  for vancomycin, and  $17.57\% \pm 11.08\%$  for doxepin hydrochloride. In accordance with adhesive results shown in Table 2, unloaded NPs showed the highest adhesive properties. The adhesive characteristics displayed a decrease for both NP-doxepin and NP-vancomycin after 4 h. Nevertheless, NP-doxycycline exhibited higher adhesive properties afterwards 4 h. Finally, all NPs exposed to mucin reduced their  $\zeta$ -potential. Unloaded and loaded NPs showed a negative surface charge. ( $-15 \pm 0.77$  mV,  $-15.75 \pm 0.79$ ,  $-18 \pm 0.70$ , and  $-15.56 \pm 1.05$  mV for unloaded NP, NP-doxepin, NP-vancomycin, and NP-doxycycline, respectively).

## 3.2 | Topography

Roughness and contact angle values are shown in Table 3.  $R_a$  was similar for the three surfaces. Polyvinyl alcohol and polyvinyl alcohol loaded with chitosan NPs film obtained similar  $R_q$  values but higher than Ti.  $R_{sk}$  was almost 0 for Ti but significantly negative for PVA and PVANP.  $R_{ku}$  was close to 3 for Ti and very platikurtic for PVA and PVANP film.  $R_p$  was similar for all three surfaces. However,  $R_v$  and  $R_{max}$  were similar for PVA and PVANP film but higher than values obtained on Ti surface. Ti, PVA, and PVANP film exhibited similar wettability. Figure 2 shows the 3D topographic profile of the surfaces studied.

## 3.3 | SEM

Figure 3A shows an isolated NP with a well-defined spherical appearance without the presence of agglomeration of particles. Figure 3B shows the uniformity of polyvinyl alcohol film. Figure 3C shows a polyvinyl alcohol loaded with chitosan NPs film. NPs alone are spherical in shape, while NPs incorporated into the PVA matrix have a less defined appearance. This could be because they are included in the structure of polyvinyl alcohol biofilm, which could give uniformity when they adhere to the NP. The biofilm rupture is possible due to the treatment received prior to the SEM technique.



**TABLE 1** Hydrodynamic diameter,  $\zeta$ -potential and PDI of NPs system.

Nanoparticle	Hydrodynamic diameter (nm)	$\zeta$ -potential (mV)	PDI
NP	354.57 (86.29)*	48.12 (7.23)*	0.556 (0.17)*
NP-doxepin	334.30 (98.15)	46.05 (9.25)	0.498 (0.13)
NP-vancomycin	349.48 (90.29)	51.90 (2.75)*	0.557 (0.13)
NP-doxycycline	804.64 (121.83)*	47.10 (3.69)	0.646 (0.21)*

Note: Equality of variances was analyzed with Fisher's test. Comparison between unloaded and loaded NP was determined by student's t-test. All measurements are expressed with their standard deviations.  $n = 3$ .

Abbreviations: NP, nanoparticle; PDI, polydispersity index.

\*Statistically significant difference ( $p < 0.05$ ).

**TABLE 2** Percentage of mucoadhesion of microparticles with and without drug with each of the drugs studied.

Time	NP	NP-doxepin	NP-vancomycin	NP-doxycycline
60	36.19 (1.47)	33.91 (0.28)	34.64 (9.87)	32.45 (1.40)
120	36.99 (3.87)	32.23 (1.37)	33.44 (9.71)	32.42 (1.09)
180	34.38 (2.91)	29.63 (1.16)	29.26 (11.27)	31.79 (0.30)
240	35.69 (2.05)	27.98 (6.38)	32.08 (3.63)	33.51 (0.05)

Note: Time is expressed in minutes. All measurements are expressed in millivolts (mV) with their standard deviations.  $n = 3$ .

Abbreviation: NP, nanoparticle.

**TABLE 3** Roughness parameters and contact angle [mean(SD)].

Surfaces	$R_p$ ( $\mu\text{m}$ )	$R_v$ ( $\mu\text{m}$ )	$R_a$ ( $\mu\text{m}$ )	$R_q$ ( $\mu\text{m}$ )	$R_{\text{max}}$ ( $\mu\text{m}$ )	$R_{\text{sk}}$ (–)	$R_{\text{ku}}$ (–)	Contact angle (degrees)
Ti	1.11 (0.28)	–1.06 (0.59)*	0.20 (0.05)	0.25 (0.05)*	2.17 (0.50)*	–0.19 (0.08)*	3.08 (0.94)*	54 (4)
PVA	1.31 (0.69)	–9.51 (4.22)	0.20 (0.05)	0.43 (0.13)	10.81 (3.77)	–15.51 (8.03)	304.23 (239.51)	54 (2)
PVANP	1.52 (0.58)	–9.20 (2.81)	0.22 (0.02)	0.39 (0.13)	11.79 (2.44)	–13.58 (4.96)	313.58 (170.5)	52 (2)

Note: Maximum relative height ( $R_p$ ), maximum relative depth ( $R_v$ ), arithmetic mean roughness ( $R_a$ ), root mean square roughness ( $R_q$ ), absolute height between the deepest valley and the highest peak ( $R_{\text{max}}$ ), the skewness ( $R_{\text{sk}}$ ), and kurtosis ( $R_{\text{ku}}$ ).  $n = 6$ .

Abbreviations: Ti, titanium; PVA, polyvinyl alcohol film; PVANP, polyvinyl alcohol loaded with chitosan nanoparticles film; SD, standard deviation.

\*Statistical difference ( $p < 0.05$ ).

### 3.4 | Drug delivery assay

Neither adsorption nor drug release occurred on the polished titanium surface. Release profile of DDs displayed two phases (Figure 4). During the first 60 min, more than 60% of drug release was detected in the PVA systems, which was considered the quick-release phase. Afterward, system showed a sustained and slow release over the time, and at this point, the second release phase was considered. PVA-doxycycline presented the slowest release profile, reaching its maximum peak at 300 min, followed by PVA-vancomycin whose peak was at 120 min. However, although the PVA-doxepin system reached more than 95% release at 60 min it was possible to detect the remaining drug at 300 min, thus reaching its maximum peak at this point.

In contrast, the combined systems exhibited a prolonged drug release. The initial rapid-release phase was observed within the first 90 min, followed by a slow-release phase for PVANP-vancomycin, PVANP-doxycycline, and PVA-doxepin which reached their peak at 360, 300, and 360 min, respectively. Finally, although the PVANP-doxepin system reached its peak at

360 min, this was the lowest release percentage, around 70%. After reaching the maximum dose release, the drugs were not detected in the media.

### 3.5 | Antimicrobial activity

The results of the  $\text{Log}_{10}$  (CFUs) are shown in Table 4. The Ti and the unloaded PVA and PVANP groups showed the highest bacterial values at 4 and 24 h with no differences between them ( $p > 0.05$ ). After 4 h, the PVA and PVANP groups loaded with vancomycin and doxycycline exhibited lower viable bacteria on their surface, being the PVANP-doxycycline the one that showed the lowest CFU counts ( $p < 0.05$ ). The groups PVA-doxepin and PVANP-doxepin gave intermediate results that were not different to the unloaded groups. Overall, the antimicrobial activity was reduced after 24 h, all groups showed a significant increase in CFUs respect to after 4 h with similar values, except for the PVA-doxycycline group, which sustained its antibiotic effect and exhibited a significantly lower CFU counts.

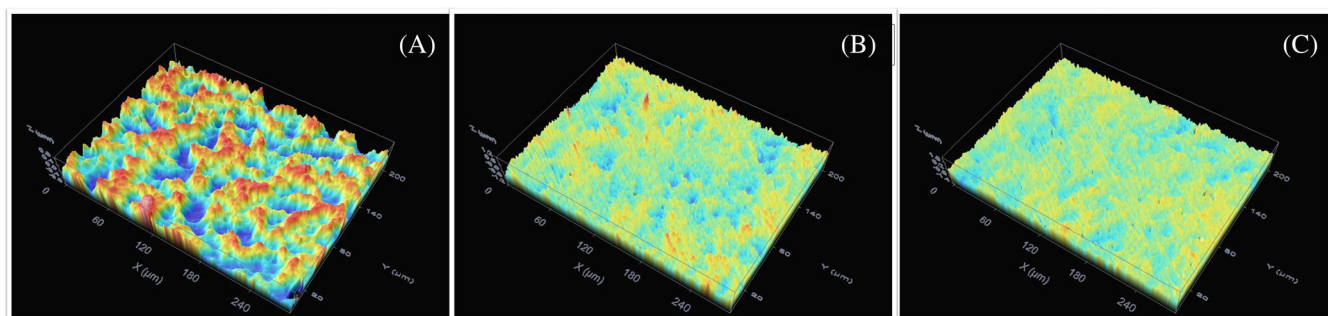


**FIGURE 2** Topographic images of the analyzed titanium surfaces. (A) Ti; titanium surface (B) PVA; Titanium surface + polyvinyl alcohol (C) PVANP; Titanium surface + polyvinyl alcohol + nanoparticles.

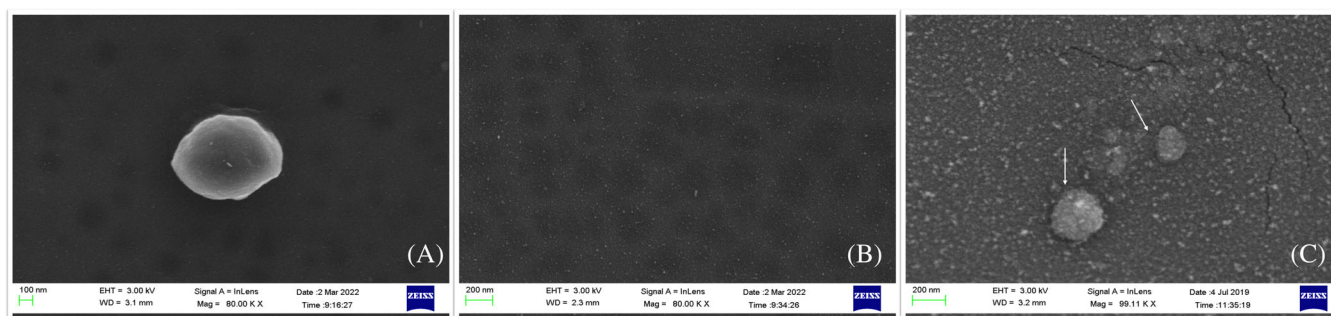


**FIGURE 3** Illustrative SEM images of drug delivery systems. (A) Chitosan bases nanoparticle (B) PVA; Titanium + polyvinyl alcohol surface (C) PVANP; Titanium + Polyvinyl alcohol + nanoparticles surface.

A similar behavior was observed in the ATP assay after 4 h (Table 5). The Ti group showed the lowest antimicrobial activity followed by the unloaded groups (PVA and PVANP). These later two groups showed comparable results to the doxepin-loaded surfaces, with no significant differences between them. The highest antimicrobial effect was observed in the PVANP-doxycycline group, followed by the PVA-vancomycin, PVANP-vancomycin, and PVA-doxycycline groups ( $p < 0.05$ ). After 24 h, the PVA-doxycycline was the only group that maintained its antimicrobial effect. The other groups gave higher RLU values, indicating the loss of their antimicrobial effect.

Table 6 shows the Live cell biovolume results. In the CLSM analysis, the Ti surface showed the highest biovolume of intact membrane cells followed by the PVANP and PVA ( $p < 0.05$ ) after 4 h. The biovolumes were significantly reduced in the loaded groups that showed a similar activity with no differences between them. After 24 h, the Ti and the unloaded PVA gave significantly higher numbers of membrane-intact bacteria. PVANP-vancomycin, exerted the highest antimicrobial activity, followed by the rest of the loaded surfaces ( $p > 0.05$ ). Figure 5. Biofilm characterization is shown in Figure 6.

## 4 | DISCUSSION

This study resulted in the successful development of a novel surface by utilizing PVA as a matrix for drug and drug-loaded NP vehiculation.

The systems developed exhibited a uniform and homogeneous matrix, with well-distributed size and appropriate surface charge for NPs. The surface coated with polyvinyl alcohol and polyvinyl alcohol loaded with chitosan NPs films demonstrated significantly less surface irregularity than the surface of the machined titanium. These findings suggest that this new surface could be a promising alternative for preventing bacterial adhesion and biofilm formation during the initial hours.

The size and distribution of NPs are considered important factors that may condition the stability, drug loading, and drug release.<sup>46</sup> Both parameters can be altered by changes in the ratio between chitosan and TPP, as well as the degree of acetylation and molecular weight of chitosan.<sup>24</sup> These changes can modify the size, and  $\zeta$ -potential and altering the internal structure and morphology of NP.<sup>13,23</sup> Affecting its load capacity and the ability to penetrate or not target tissues.<sup>46</sup> Consequently, the biological fate, targeting efficacy, toxicity, and in vivo distribution of delivery systems are affected.<sup>46</sup> Optimizing NP size can lead to higher drug release at the desired site, which can result in enhanced therapeutic efficacy.<sup>11</sup> That is why it is crucial to optimize these parameters to achieve optimal performance of NP-based delivery systems.

It has been demonstrated that modifying the pH, Cs:TPP ratio, and acetic acid ratio during the synthesis of chitosan NPs affects the characteristics of the system.<sup>23,24,47</sup> De Pinho and colleagues (2014) revealed that an increase in the concentration of Cs:TPP resulted in a



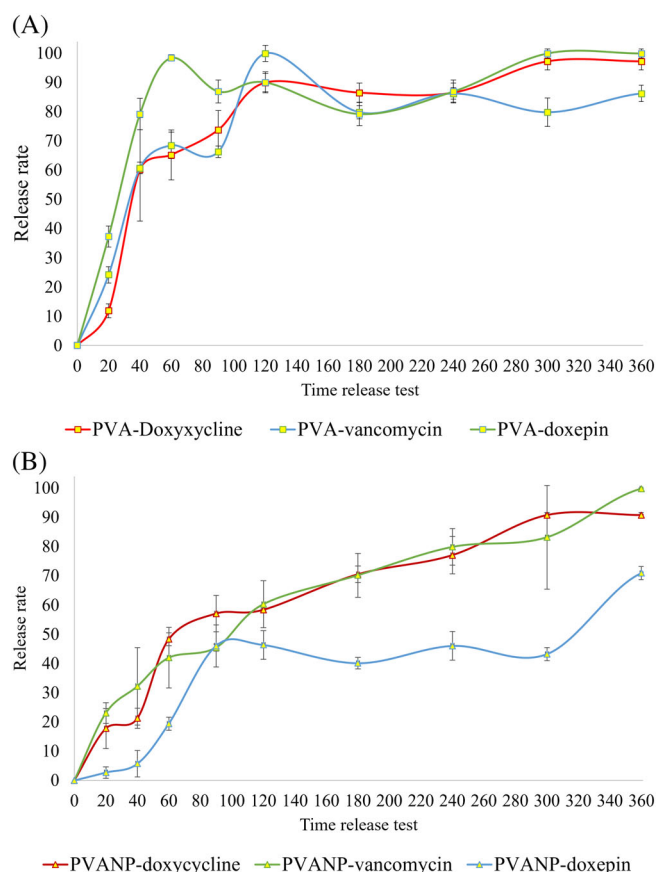


**FIGURE 4** In vitro drug release profile of drug delivery systems. Release rate is expressed in percentage (%). Time is expressed in minutes. (A) Drug release profile of PVA films. (B) Drug release profile of PVANP films.

larger NP size (508.1 nm) with a higher surface charge (57.3 mV).<sup>23</sup> Quan Gan and colleagues (2005) showed that particle size and  $\zeta$ -potential increased when the Cs:TPP ratio was higher. However, it was reported that a higher chitosan concentration caused an increase in NP size but a decrease in their  $\zeta$ -potential.<sup>24</sup> Pawar and colleagues (2018) reported larger sizes and surface charges as the Cs:TPP concentration increased. The Cs:TPP concentration at 0.1%:0.5% presented a particle diameter of  $276.4 \pm 16.48$  nm and  $\zeta$ -potential of  $37.13 \pm 3.18$  mV while a concentration at 0.2% and 0.5% obtained a size of  $389 \pm 13.15$  and a  $\zeta$ -potential of  $63.42 \pm 3.21$  mV.<sup>47</sup> These results highlight the importance of the NP size and  $\zeta$ -potential in their biological behavior, as well as the significant impact of the Cs:TPP ratio on the properties of NP. In addition, it has been reported that NP with a  $\zeta$ -potential above 30 mV tend to have improved stability and reduced aggregation tendency.<sup>23,46,48</sup> The stability test conducted in this study also demonstrated that the NP systems maintained a  $\zeta$ -potential above 30 mV for a period of 45 days, indicating their stability in all cases. Furthermore, although NP-doxycycline showed the higher diameter the size of the NPs was deemed appropriate in all cases as the aim was not to achieve systemic effects or NP permeation into the tissue. Instead, the main objective was to achieve a localized effect and a controlled release at the administration site.

The size of NP also plays a key role in DEE% and in consequence drug release is affected by particle size. Since large particles have the capacity to encapsulate more drug because they have large cores compared to smaller one.<sup>46</sup> A high percentage of drug encapsulation efficiency is essential to optimize the release profile. Based on Azizian and colleagues (2018) developed a Cs NP system with basic fibroblast growth factor and bovine serum albumin (BSA), in which  $20\% \pm 1.2\%$  of BSA was successfully encapsulated. The system showed a release rate of 80% within the first 4 h, indicating efficient release kinetics.<sup>49</sup> In the same way, Cover and colleagues (2012) studied two particle formulation to encapsulate doxycycline into chitosan NP (DCNP), achieving an encapsulation of  $53\% \pm 19\%$  and  $56\% \pm 10\%$  for DCNP4 and DCNP6, respectively. DCNP4 showed a burst effect within the first 5 h ( $<60\%$ ) while DCNP6, within the first 4 h ( $>60\%$ ).<sup>13</sup> Pawar and colleagues (2018) reported an encapsulation efficiency of vancomycin between  $46.4\% \pm 2.1\%$  and  $65.3\% \pm 1.9\%$  for particle size between 276 and 389 nm.<sup>47</sup> This suggests that encapsulation efficiency varies as a function of solution pH, as well as Cs:TPP concentration and polymer/drug ratio.<sup>47</sup>

On the other hand, Castán and colleagues (2015) investigated the release profile of doxepin hydrochloride from three different biofilms over a 6-h period (chitosan, hydroxypropyl methyl cellulose, and carboxymethyl cellulose). The results showed that the release behavior of hydroxypropyl methyl cellulose and chitosan biofilms was similar, with both exhibiting an initial rapid release followed by a sustained release over 6 h. In the first hour, chitosan achieved a release profile around 43%, HPMC achieved 38%, and SCMC achieved 19%.<sup>14</sup> Yang and colleagues (2018) designed a PVA/Cs liquid film-forming system (LFFS) to deliver benzalkonium bromide (BZL). BZL release showed different values as PVA concentration increased. LFFS (0% PVA and 1% Cs) reached 90% release at 36 h, whereas LFFS (10% PVA and 1% Cs) took 60 h to reach 90% release.<sup>33</sup> The release behavior can be explained by the biodegradability of the material. When polyvinyl alcohol matrix reaches contact with the medium, the erosion and biodegradation of the biofilm begins, which corresponds to the system's rapid release phase.<sup>17</sup> This is followed by the sustained release phase, in which the system needs to degrade completely to release the remaining drug. This behavior is delayed when the NPs are in the PVA matrix, as the biofilm serves as a protective barrier. Once the NPs are released from the matrix, drug release begins. In addition, drug solubility and diffusion in or across the polymer become a determining factor in drug release.<sup>46</sup>

Having a thorough understanding of a material's adhesive properties can be a valuable strategy to predict and plan the polymer's attachment to the desired site. Vieira and colleagues (2018) compared solid lipid nanoparticles (SLNs) with chitosan-coated SLNs (C-SLNs) in terms of their mucin adhesion properties. The results revealed that C-SLNs exhibited higher mucin adhesion than SLNs.<sup>40</sup> An ionic interaction occurs when the positively charged amino group of chitosan comes into contact with the negatively charged carboxyl and sulfate groups of Mucin.<sup>11,40</sup> This interaction results in a change in size,  $\zeta$ -potential, and PDL. The adhesive properties of NP were validated by observing changes in particle size and zeta potential following the

Surfaces		Log <sub>10</sub> CFUs		Comparison <i>p</i> -value**
		4 h	24 h	
		Median (IR)	Media (IR)	
Ti		6.38 (1.35) <sup>a</sup>	7.32 (0.52) <sup>a</sup>	0.004
PVA	Unloaded	5.58 (0.68) <sup>a</sup>	7.57 (0.48) <sup>a</sup>	<0.001
	Doxepin	5.34 (1.17) <sup>a,b</sup>	7.70 (0.55) <sup>c</sup>	<0.001
	Vancomycin	4.59 (1.15) <sup>c</sup>	6.84 (0.66) <sup>b</sup>	<0.001
	Doxycycline	4.63 (2.17) <sup>c</sup>	3.71 (0.73) <sup>c</sup>	0.063
PVANP	Unloaded	5.53 (1.44) <sup>a,b</sup>	7.30 (0.70) <sup>a</sup>	<0.001
	Doxepin	5.40 (2.20) <sup>a,b</sup>	7.45 (0.73) <sup>a</sup>	<0.001
	Vancomycin	4.70 (1.40) <sup>c</sup>	6.92 (0.16) <sup>a</sup>	<0.001
	Doxycycline	3.90 (1.23) <sup>d</sup>	6.92 (0.66) <sup>a</sup>	<0.001
Comparison of <i>p</i> -value*		<0.001	<0.001	

Abbreviations: CFU, colony-forming units; IR, interquartile rank; PVA, polyvinyl alcohol; PVANP, polyvinyl alcohol loaded with chitosan nanoparticle.

\*Multiple comparisons by Kruskal–Wallis test. Within each column, the same superscript lowercase letter shows not statistical differences by Mann–Whitney test.

\*\*Comparisons 4 versus 24 h by Mann–Whitney test.

**TABLE 4** Results of the Log<sub>10</sub> of the colony-forming units were obtained with each of the study groups after 4 and 24 h.

Surfaces		Relative light units		Comparison <i>p</i> -value**
		4 h	24 h	
		Median (IR)	Median (IR)	
Ti		12.799 (32.760,75) <sup>a</sup>	34.724,5 (58.926,38) <sup>a</sup>	0.043
PVA	Unloaded	6.176 (5.609,25) <sup>a,b</sup>	90.903 (80.839,63) <sup>a</sup>	<0.001
	Doxepin	3344 (7376) <sup>b,c</sup>	80999 (155193) <sup>a</sup>	<0.001
	Vancomycin	2218 (2644) <sup>c</sup>	161189 (306817) <sup>a</sup>	<0.001
	Doxycycline	4811 (6238) <sup>c</sup>	1611 (2615) <sup>b</sup>	0.105
PVANP	Unloaded	5615 (11551) <sup>b</sup>	40880 (57704) <sup>a</sup>	<0.001
	Doxepin	56035 (23833) <sup>b,c</sup>	103059 (88132) <sup>a</sup>	<0.001
	Vancomycin	2281 (4460) <sup>c,d</sup>	99911 (142675) <sup>a</sup>	<0.001
	Doxycycline	1624 (1727) <sup>d</sup>	68366 (81431) <sup>a</sup>	<0.001
Comparison of <i>p</i> -value*		0.002	<0.001	<0.001

Abbreviations: IR, interquartile rank; PVA, polyvinyl alcohol; PVANP, polyvinyl alcohol loaded with chitosan nanoparticle.

\*Multiple comparisons by Kruskal–Wallis test. Within each column, the same superscript lowercase letter shows not statistical differences by Mann–Whitney test.

\*\*Comparisons 4 versus 24 h by Mann–Whitney test.

**TABLE 5** Results of the relative light units obtained with the ATP test with each of the study groups after 4 and 24 h.

interaction described above. These changes provided evidence of the adhesive nature of the particles.

Topography and wettability were measured to control if they were determining factors in bacterial activity. Topography and surface wetting condition the biofilm formation. Bioactive surfaces have reduced antibacterial effect.<sup>8</sup> The main concern about antifouling surfaces is the possible negative impact for initial protein adsorption and, importantly, for host cell adhesion processes.<sup>8</sup> Thus, smoothening the surface can reduce biofilm formation, and a Ra roughness values close to 0.2 µm was reported to be the threshold for maximum reduction of bacterial

adhesion on abutment surfaces.<sup>50</sup> In this work,  $R_a$  was close to this critical value. Although there are some parameters with differences between groups, topography effect was minimized. Regards wetting, the effect was not significant to the biofilm formation, because bacterial activity was similar on the Ti and PVA film surfaces without drug loading. The drug did not influence the contact angle values. Then, the surface effect on the bacteria activity is only focused on the drug and NP effect and not on the topography or wetting characteristics.

For the antimicrobial activity, a multiple-species biofilm was used from dental plaque because it is closer to the in vivo situation than a

**TABLE 6** Live cell biovolume results of the study groups after 4 and 24 h.

		Biovolume $\mu\text{m}^3$		Comparison of $p$ -value**
		4 h	24 h	
Surfaces		Median (IR)	Median (IR)	
Ti		10128 (15 979) <sup>a</sup>	67381 (60 214) <sup>a</sup>	<0.001
PVA	Unloaded	1662 (1349) <sup>b</sup>	65774 (17 649) <sup>a</sup>	<0.001
	Doxepin	830 (515) <sup>c</sup>	29233 (33 742) <sup>b</sup>	<0.001
	Vancomycin	1157 (940) <sup>c</sup>	7491 (14895) <sup>c</sup>	<0.001
	Doxycycline	471 (439) <sup>c</sup>	857 (1288) <sup>c</sup>	0.482
PVANP	Unloaded	5881 (1626) <sup>b,c</sup>	11951 (24 103) <sup>d</sup>	0.031
	Doxepin	573 (2254) <sup>c</sup>	11995 (7089) <sup>d</sup>	<0.001
	Vancomycin	1091 (1225) <sup>c</sup>	73 (23) <sup>e</sup>	<0.001
	Doxycycline	7218720 (1525) <sup>c</sup>	3177 (14192) <sup>c</sup>	0.002
Comparison of $p$ -value*		<0.001	<0.001	

Abbreviations: IR, interquartile rank; PVA, polyvinyl alcohol; PVANP, polyvinyl alcohol loaded with chitosan nanoparticle.

\*Multiple comparisons by Kruskal–Wallis test. Within each column, the same superscript lowercase letter shows not statistical differences by Mann–Whitney test.

\*\*Comparisons 4 versus 24 h by Mann–Whitney test.

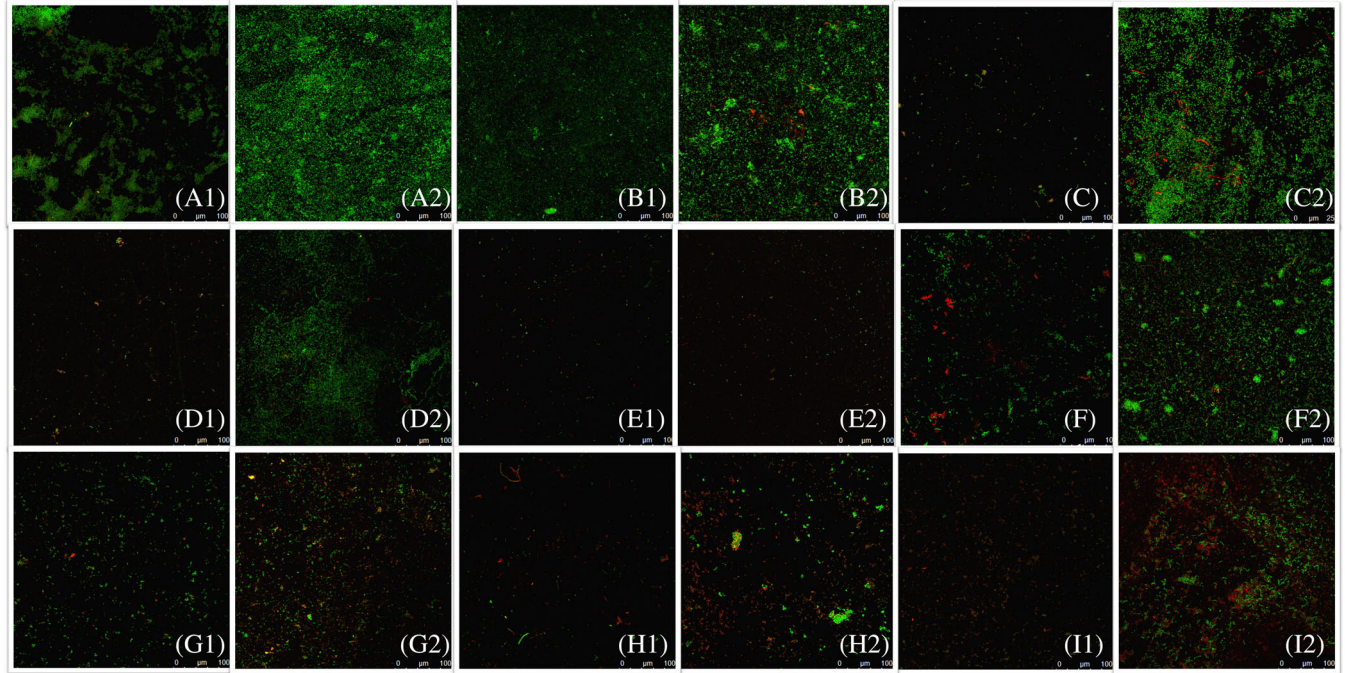


**FIGURE 5** Representative confocal laser scanning microscopy images of natural multispecies biofilms grown on the surface of the different study groups: (A) Ti, (B) PVA, (C) PVADH, (D) PVAVx, (E) PVADox (F) PVANP (G) PVANP DH, (H) PVANP Vx, (I) PVANP Dox. (1) Samples exposed 4 h. (2) Samples exposed 24 h. Green-colored bacteria are cells with intact membranes and red-colored bacteria are cells with damaged membranes following live/dead staining (BacLight; Invitrogen, Eugene, OR, USA).

single-species biofilm.<sup>19,51,52</sup> Different methods were employed to test antimicrobial activity of the DDs as there is no gold standard technique.<sup>43</sup> CFU recovers viable microorganisms but it does not detect viable but non-culturable bacteria (VBNC), resulting in miscalculation in oral biofilms-around 50% of the oral population is in this

VBNC state.<sup>43</sup> On the contrary, the ATP assay quantifies the microbial ATP production of the whole community including viable and VBNC bacteria.<sup>43,51,53</sup> However, the amount of ATP generated could differ depending on the species, and therefore estimating the microbial cell count in a multispecies biofilm can be challenging.<sup>51</sup> CLSM and the



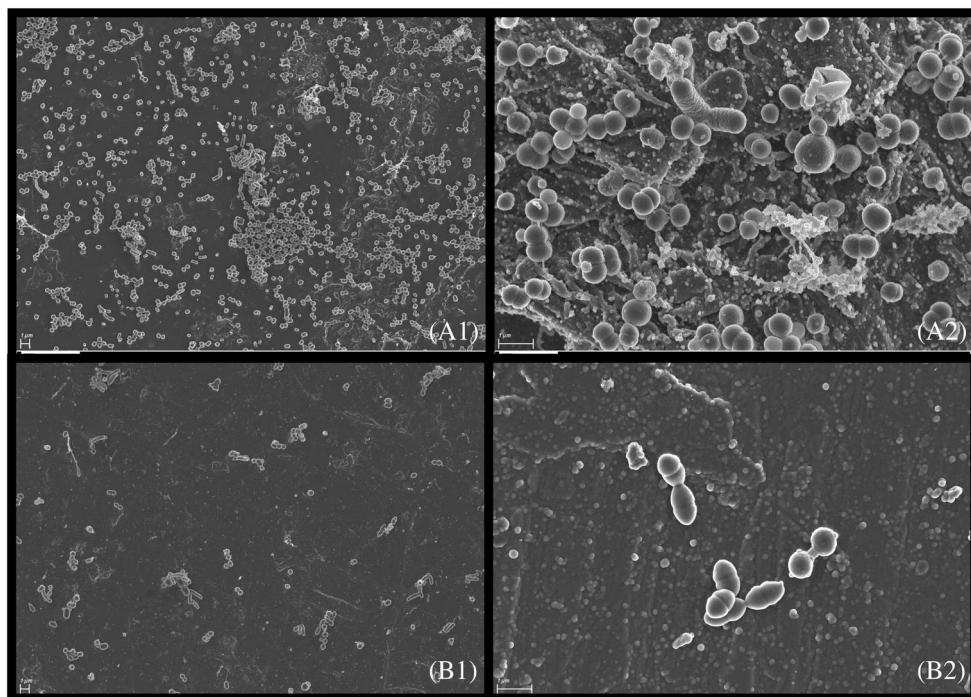


**FIGURE 6** Illustrative SEM images of two surfaces with different bacterial inhibition. (A) Low inhibition. (B) High inhibition. (1) Original magnification  $\times 5000$ . (2) Original magnification  $\times 20\,000$ .

LIVE/DEAD technique were furthermore included because it classifies the cells according to the state of the membrane so that intact-membrane bacteria could be considered alive and damaged cells as dead. The main limitation of this technique is that intact membrane cells can be metabolically inactive, thus dead, whereas damaged membrane cells may still be alive, leading to false results.<sup>43,53</sup>

The antimicrobial activity of the films was tested after 4 and 24 h since maintaining a controlled release of dosage within the first hours is crucial to ensure an aseptic environment with the aim of preventing bacterial adhesion.<sup>47</sup> According to Hetrick and colleagues (2006), there is a “decisive period” after implantation during which preventing bacterial adhesion is critical for ensuring the long-term success of an implant.<sup>6</sup> Despite the polyvinyl alcohol and polyvinyl alcohol loaded with chitosan NPs films were dissolved, and the drugs released within the first 6 h, the films were evaluated after 24 h to verify the effects of any residual drug in the medium term and its effects on bacteria.

Overall, the results of the CFU, ATP, and CLSM assays were consistent for the different study groups. As expected, bacterial growth was not inhibited by titanium disks, and similar results were obtained in samples coated with a PVA film, as shown in a previous study.<sup>19</sup> However, when drug-free NPs were loaded into the PVA film, some activity was observed. Chitosan has shown antibiofilm activity and the capacity to inhibit the bacterial adhesion to the surface.<sup>13,33,48,54</sup> This property is conferred by the molecular weight, concentration, and polycationic nature of chitosan, due to the presence of functional amino groups ( $\text{NH}_2$ ) in N-acetylglucosamine units.<sup>48,55</sup> Chitosan interacts with negatively charged biofilm components, such as extracellular polymeric substances (EPS) and the cell wall, resulting in an increased permeability of the cell surface membrane, facilitating bacterial components leakage.<sup>48,54–57</sup>

Bacterial inhibition was increased when the polyvinyl alcohol and polyvinyl alcohol loaded with chitosan NPs films were loaded with the antibiotics. Doxycycline exerted a higher antibacterial activity and with a longer effect than vancomycin, especially the PVANP-doxycycline group. This tetracycline has a broad-spectrum activity and is effective against gram-positive and gram-negative bacteria, as well as spirochetes and mycoplasmas.<sup>12,13</sup> Its action mechanism is associated with inhibition of protein synthesis.<sup>57,58</sup> Vancomycin, in contrast, is a glycopeptide antibiotic that inhibits bacterial cell wall synthesis<sup>47</sup> and is particularly effective against gram-positive bacteria such as *Staphylococcus aureus*, commonly found in implant-associated infections.<sup>47,59</sup> Despite its benefits, vancomycin has some drawbacks, such as the development of resistance in gram-negative organisms related to the inability of the drug to penetrate the bacterial outer membrane barrier.<sup>60</sup> Although with no significant differences, after 4 h the PVANP-doxycycline y PVANP-vancomycin gave better results than the PVA-doxycycline and PVA-vancomycin films. A possible explanation could be that once the NPs are released from the PVA film, they adhere to the cell wall altering the permeability and leaving the bacteria more susceptible to the presence of the antibiotic. Interestingly, the PVANP-doxycycline gave significantly lower RLUs than CFUs. It is possible that the bacterial metabolism was more affected in this group although the bacteria were still alive.

The lowest microbial count and ATP production at 4 h were observed with the PVANP-doxycycline sample, followed by PVA-vancomycin, PVANP-vancomycin, and PVA-doxycycline. The efficacy of almost all systems was reduced after 24 h which can be a consequence of the fact that the drug's release occurs within the first 6 h, as observed in the release assay. In addition, the dose and the amount

of chitosan particles incorporated in the systems could have also influenced this effect. The reduction of the antimicrobial agent overtime might have allowed bacteria to grow on the coated titanium surfaces. Furthermore, the more mature the biofilm is, the more resistant it becomes to the action of residual antimicrobials as a consequence of several mechanisms such as the development of the EPS matrix and other factors such as the presence of persisted cells.<sup>43,52</sup> After 24 h the PVA-doxycycline was the only system that maintained its antibacterial effect. This activity overtime can be related to a longer post antibiotic effect (PAE)-the time expressed in hours that bacteria take to recover their normal growth after the antibiotic exposure- of doxycycline compared to vancomycin.<sup>58</sup> In fact, the PAEs of doxycycline encapsulated in NPs against two strains of methicillin-resistant *Staphylococcus aureus* (MRSA), MRSA-S1 and MRSA-S2, were 3 and 3.5 h, respectively.<sup>58</sup> In contrast, vancomycin PAE was shown to be shorter against MRSA between 1 and 2 h, which could justify the loss of activity after 6 h. Finally, the effectiveness of the PVA-doxycycline system after 24 h can also be attributed to the higher therapeutic dose of the drug when it is integrated into the PVA matrix compared to the NP (124.80 µg in PVA-doxycycline vs. 67.01 µg in the PVANP-doxycycline).

Surprisingly, the antibacterial activity of doxepin hydrochloride was very low, especially when it was loaded into PVA film. Doxepin hydrochloride, a dibenzoxepin-derivate tricyclic antidepressant (TCAs) has been used as an alternative treatment to non-steroidal anti-inflammatory drug for dermal or mucosal pain control because of its local analgesic and anesthetic properties in small doses.<sup>14,15,61</sup> Moreover, TCAs have shown antifungal and antimicrobial effects on intestinal pathogens such as *Escherichia coli*, *Yersinia enterocolitica*, and *Giardia lamblia*.<sup>62–64</sup> The mechanism of action of TCAs against bacteria is not well understood. It has been reported that some post-selective serotonin reuptake inhibitors exert dual action as serotonin and norepinephrine reuptake inhibitors, this is a property also possessed by one or more of the TCAs, such as doxepin hydrochloride.<sup>65,66</sup> Some hypotheses suggest that TCAs inhibit DNA plasmid replication and the DNA gyrase enzyme, as well as bacterial efflux pump.<sup>62–64</sup> Additionally, drugs with two or more benzene rings in their chemical structure have been reported to possess antimicrobial activity.<sup>67</sup> The serotonin and norepinephrine reuptake mechanism of doxepin hydrochloride,<sup>14,66</sup> as well as its chemical structure with two benzene rings, may be responsible for its bacteriostatic effect.

Furthermore, by incorporating NPs into the PVA hydrogel matrix, we can achieve targeted drug delivery to specific sites, such as infected tissues. The development of this DDs can provide new opportunities for the treatment of various diseases and may lead to significant improvements in patient outcomes.

Finally, the present study has several limitations. The antimicrobial activity was evaluated by culture technique which shows limitations as it cannot recover all the microorganisms in a natural sample, and it does not provide information about the taxonomic composition of the biofilm. Further studies using sequencing techniques and conditions that are closer to the clinical scenario should be conducted.

## 5 | CONCLUSIONS

Polyvinyl alcohol film has been shown to be an effective matrix for transporting drugs and chitosan NPs. In addition, chitosan particles are a stable system over time and with the ability to carry drugs. Polyvinyl alcohol film has adequate adhesive properties, and its easy preparation is an interesting option for loading and modifying titanium implant surfaces. Among the drugs evaluated, doxycycline was the most effective against bacteria and with a more prolonged effect.

## AUTHOR CONTRIBUTIONS

**Pablo Yael Carrazco Ávila:** Conceptualization, Methodology, Investigation, and Writing—original draft, Writing—review and editing. **Teresa Arias Moliz:** Conceptualization, Methodology, Investigation, Resources, Supervision and Writing—review and editing. **Juan Ignacio Rosales Leal:** Conceptualization, Methodology, Investigation, Resources, Supervision, Writing—original draft and Writing—review and editing. **Pilar Baca:** Validation, and statistical analysis. **Miguel Ángel Rodríguez Valverde:** Validation, Resources, and statistical analysis. **María Encarnación Morales Hernandez:** Conceptualization, Methodology, Investigation, Resources, Supervision, Writing—original draft, and Writing—review and editing.

## ACKNOWLEDGMENTS

Pablo Yael Carrazco-Ávila thanks the Autonomous University of Sinaloa (México) for the financial support provided for his studies in the doctoral program in clinical medicine and Public Health taught by the University of Granada (Spain). The authors would like to thank Francisca Castillo Perez for her technical assistance. The authors also thank Project PID2020.116082GB-I00 (MCIN/AEI/10.13039/501100011033), Project C-CTS-305-UGR23 (University of Granada, Spain) and the research group CTS-974 (Junta de Andalucía, Spain) for the economic support. Funding for open access charge: Universidad de Granada / CBUA.



## CONFLICT OF INTEREST STATEMENT

The authors declare no conflicts of interest.

## DATA AVAILABILITY STATEMENT

The data that support the findings of this study are available from the corresponding author upon reasonable request.

## ORCID

Pablo Yael Carrazco Ávila  <https://orcid.org/0000-0001-8638-6001>  
Juan Ignacio Rosales Leal  <https://orcid.org/0000-0002-4575-4098>

## REFERENCES

- Albrektsson T, Brånemark PI, Hansson HA, Lindström J. Osseointegrated titanium implants: requirements for ensuring a long-lasting, direct bone-to-implant anchorage in man. *Acta Orthop Scand*. 1981; 52(2):155–170. doi:[10.3109/17453678108991776](https://doi.org/10.3109/17453678108991776)
- Botticelli D, Berglundh T, Buser D, Lindhe J. The jumping distance revisited: an experimental study in the dog. *Clin Oral Implants Res*. 2003;14(1):35–42. doi:[10.1034/j.1600-0501.2003.140105.x](https://doi.org/10.1034/j.1600-0501.2003.140105.x)



3. Le GL, Soueidan A, Layrolle P, Amouriq Y. Surface treatments of titanium dental implants for rapid osseointegration. *Dent Mater.* 2007; 23(7):844-854. doi:[10.1016/j.dental.2006.06.025](https://doi.org/10.1016/j.dental.2006.06.025)
4. Pellegrini G, Francetti L, Barbaro B, Fabbro M. Novel surfaces and osseointegration in implant dentistry. *J Invest Clin Dent.* 2018;9:1-9. doi:[10.1111/jicd.12349](https://doi.org/10.1111/jicd.12349)
5. Xing H, Wang X, Xiao S, et al. Osseointegration of layer-by-layer polyelectrolyte multilayers loaded with IGF1 and coated on titanium implant under osteoporotic condition. *Int J Nanomedicine.* 2017;12: 7709-7720. doi:[10.2147/IJN.S148001](https://doi.org/10.2147/IJN.S148001)
6. Hetrick EM, Schoenfish MH. Reducing implant-related infections: active release strategies. *Chem Soc Rev.* 2006;35(9):780-789. doi:[10.1039/B515219B](https://doi.org/10.1039/B515219B)
7. Zhao L, Chu PK, Zhang Y, Wu Z. Antibacterial coatings on titanium implants. *J Biomed Mater Res Part B Appl Biomater.* 2009;91B(1):470-480. doi:[10.1002/jbm.b.31463](https://doi.org/10.1002/jbm.b.31463)
8. Barão VAR, Costa RC, Shibli JA, Bertolini M, Souza JGS. Emerging titanium surface modifications: the war against polymicrobial infections on dental implants. *Braz Dent J.* 2022;33(1):1-12. doi:[10.1590/0103-6440202204860](https://doi.org/10.1590/0103-6440202204860)
9. Chourirfa H, Bouloussa H, Migonney V, Falentin-Daudré C. Review of titanium surface modification techniques and coatings for antibacterial applications. *Acta Biomater.* 2019;83:37-54. doi:[10.1016/j.actbio.2018.10.036](https://doi.org/10.1016/j.actbio.2018.10.036)
10. Akshaya S, Rowlo PK, Dukle A, Nathanael AJ. Antibacterial coatings for titanium implants: recent trends and future perspectives. *Antibiotics.* 2022;11(12):1719. doi:[10.3390/ANTIBIOTICS11121719](https://doi.org/10.3390/ANTIBIOTICS11121719)
11. Cerchiara T, Abruzzo A, di Cagno M, et al. Chitosan based micro- and nanoparticles for colon-targeted delivery of vancomycin prepared by alternative processing methods. *Eur J Pharm Biopharm.* 2015;92:112-119. doi:[10.1016/j.ejpb.2015.03.004](https://doi.org/10.1016/j.ejpb.2015.03.004)
12. Zhou Z, Hu F, Hu S, et al. pH-activated nanoparticles with targeting for the treatment of oral plaque biofilm†. *J Mater Chem B.* 2018;586: 586-592. doi:[10.1039/c7tb02682j](https://doi.org/10.1039/c7tb02682j)
13. Cover NF, Lai-Yuen S, Parsons AK, Kumar A. Synergetic effects of doxycycline-loaded chitosan nanoparticles for improving drug delivery and efficacy. *Int J Nanomedicine.* 2012;7:2411-2419. doi:[10.2147/IJN.S27328](https://doi.org/10.2147/IJN.S27328)
14. Castán H, Ruiz MA, Clares B, Morales ME. Design, development and characterization of buccal bioadhesive films of doxepin for treatment of odontalgia. *Drug Deliv.* 2015;22(6):869-876. doi:[10.3109/10717544.2014.896958](https://doi.org/10.3109/10717544.2014.896958)
15. Laffleur F, Zilio M, Shuwisitkul D. Modified biomolecule as potential vehicle for buccal delivery of doxepin. *Ther Deliv.* 2016;7(10):683-689. doi:[10.4155/tde-2016-0046](https://doi.org/10.4155/tde-2016-0046)
16. Pawlik A, Socha RP, Hubalek Kalbacova M, Sulka GD. Surface modification of nanoporous anodic titanium dioxide layers for drug delivery systems and enhanced SAOS-2 cell response. *Colloids Surf B Biointerfaces.* 2018;171:58-66. doi:[10.1016/j.colsurfb.2018.07.012](https://doi.org/10.1016/j.colsurfb.2018.07.012)
17. Barik A, Chakravorty N. Targeted drug delivery from titanium implants: a review of challenges and approaches. *Adv Exp Med Biol.* 2020;1251:1-17. doi:[10.1007/5584\\_2019\\_447/FIGURES/5](https://doi.org/10.1007/5584_2019_447/FIGURES/5)
18. Mabrouk M, Rajendran R, Soliman IE, et al. Nanoparticle- and nanoporous-membrane-mediated delivery of therapeutics. *Pharmaceutics.* 2019;11(6):294. doi:[10.3390/PHARMACEUTICS11060294](https://doi.org/10.3390/PHARMACEUTICS11060294)
19. Hajji S, Chaker A, Jridi M, et al. Structural analysis, and antioxidant and antibacterial properties of chitosan-poly (vinyl alcohol) biodegradable films. *Environ Sci Pollut Res.* 2016;23(15):15310-15320. doi:[10.1007/S11356-016-6699-9/FIGURES/7](https://doi.org/10.1007/S11356-016-6699-9/FIGURES/7)
20. Niranjana R, Kaushik M, Prakash J, et al. Enhanced wound healing by PVA/chitosan/curcumin patches: in vitro and in vivo study. *Colloids Surf B Biointerfaces.* 2019;182:110339. doi:[10.1016/j.colsurfb.2019.06.068](https://doi.org/10.1016/j.colsurfb.2019.06.068)
21. Ding J, He R, Zhou G, Tang C, Yin C. Multilayered mucoadhesive hydrogel films based on thiolated hyaluronic acid and polyvinylalcohol for insulin delivery. *Acta Biomater.* 2012;8(10):3643-3651. doi:[10.1016/j.actbio.2012.06.027](https://doi.org/10.1016/j.actbio.2012.06.027)
22. Kazsoki A, Szabó P, Zekó R. Prediction of the hydroxypropyl cellulose—poly(vinyl alcohol) ratio in aqueous solution containing papaverine hydrochloride in terms of drug loaded electrospun fiber formation. *J Pharm Biomed Anal.* 2017;138:357-362. doi:[10.1016/j.jpba.2017.02.030](https://doi.org/10.1016/j.jpba.2017.02.030)
23. de Pinho Neves AL, Milioli CC, Müller L, Riella HG, Kuhnén NC, Stulzer HK. Factorial design as tool in chitosan nanoparticles development by ionic gelation technique. *Colloids Surf A Physicochem Eng Asp.* 2014;445:34-39. doi:[10.1016/j.colsurfa.2013.12.058](https://doi.org/10.1016/j.colsurfa.2013.12.058)
24. Gan Q, Wang T, Cochrane C, McCarron P. Modulation of surface charge, particle size and morphological properties of chitosan-TPP nanoparticles intended for gene delivery. *Colloids Surf B Biointerfaces.* 2005;44(2-3):65-73. doi:[10.1016/j.colsurfb.2005.06.001](https://doi.org/10.1016/j.colsurfb.2005.06.001)
25. Norowski PA, Courtney HS, Babu J, Haggard WO, Bumgardner JD. Chitosan coatings deliver antimicrobials from titanium implants: a preliminary study. *Implant Dent.* 2011;20(1):56-67. doi:[10.1097/ID.0b013e3182087ac4](https://doi.org/10.1097/ID.0b013e3182087ac4)
26. Bumgardner JD, Wiser R, Gerard PD, et al. Chitosan: potential use as a bioactive coating for orthopaedic and craniofacial/dental implants. *J Biomater Sci Polym Ed.* 2003;14:423-438. doi:[10.1163/156856203766652048](https://doi.org/10.1163/156856203766652048)
27. Furlani F, Sacco P, Decleva E, et al. Chitosan acetylation degree influences the physical properties of polysaccharide nanoparticles: implication for the innate immune cells response. *ACS Appl Mater Interfaces.* 2019;11(10):9794-9803. doi:[10.1021/acsami.8b21791](https://doi.org/10.1021/acsami.8b21791)
28. Almalik A, Alradwan I, Majrashi MA, et al. Cellular responses of hyaluronic acid-coated chitosan nanoparticles. *Toxicol Res.* 2018;7(5): 942-950. doi:[10.1039/c8tx00041g](https://doi.org/10.1039/c8tx00041g)
29. Fernández-Urrusuno R, Calvo P, Remuñán-López C, Vila-Jato JL, José AM. Enhancement of nasal absorption of insulin using chitosan nanoparticles. *Pharm Res.* 1999;16(10):1576-1581. doi:[10.1023/A:1018908705446](https://doi.org/10.1023/A:1018908705446)
30. Kumar MNVR, Muzzarelli RAA, Muzzarelli C, Sashiwa H, Domb AJ. Chitosan chemistry and pharmaceutical perspectives. *Chem Rev.* 2004;104(12):6017-6084. doi:[10.1021/cr030441b](https://doi.org/10.1021/cr030441b)
31. Kumar A, Vimal A, Kumar A. Why chitosan? From properties to perspective of mucosal drug delivery. *Int J Biol Macromol.* 2016;91:615-622. doi:[10.1016/j.ijbiomac.2016.05.054](https://doi.org/10.1016/j.ijbiomac.2016.05.054)
32. Li Y, Li L, Ma Y, et al. 3D-printed titanium cage with PVA-vancomycin coating prevents surgical site infections (SSIs). *Macromol Biosci.* 2020; 20(3):1900394. doi:[10.1002/mabi.201900394](https://doi.org/10.1002/mabi.201900394)
33. Yang S, Yang Y, Cui S, et al. Chitosan-polyvinyl alcohol nanoscale liquid film-forming system facilitates MRSA-infected wound healing by enhancing antibacterial and antibiofilm properties. *Int J Nanomed.* 2018;13:4987-5002. doi:[10.2147/IJN.S161680](https://doi.org/10.2147/IJN.S161680)
34. Song W, Zhao L, Fang K, Chang B, Zhang Y. Biofunctionalization of titanium implant with chitosan/siRNA complex through loading-controllable and time-saving cathodic electrodeposition. *J Mater Chem B.* 2015;3(43):8567-8576. doi:[10.1039/C5TB01062D](https://doi.org/10.1039/C5TB01062D)
35. Zahran R, Rosales Leal JL, Rodríguez Valverde MA, Cabrero Vilchez MA. Effect of hydrofluoric acid etching time on titanium topography, chemistry, wettability, and cell adhesion. *PLoS One.* 2016;11(11):e0165296. doi:[10.1371/journal.pone.0165296](https://doi.org/10.1371/journal.pone.0165296)
36. Sánchez-Treviño AY, García-Martínez O, Blasco-Avellaneda D, et al. Effect of the terminal group of phosphonate self-assembled films formed on Ti surfaces on the biomimetic layer formation and cell adhesion. *Appl Surf Sci.* 2016;362:304-314. doi:[10.1016/j.apsusc.2015.11.174](https://doi.org/10.1016/j.apsusc.2015.11.174)
37. Fan W, Yan W, Xu Z, Ni H. Formation mechanism of monodisperse, low molecular weight chitosan nanoparticles by ionic gelation technique. *Colloids Surf B Biointerfaces.* 2012;90:21-27. doi:[10.1016/j.colsurfb.2011.09.042](https://doi.org/10.1016/j.colsurfb.2011.09.042)

38. Almalik A, Alradwan I, Kalam MA, Alshamsan A. Effect of cryoprotection on particle size stability and preservation of chitosan nanoparticles with and without hyaluronate or alginate coating. *Saudi Pharm J*. 2017;25(6):861-867. doi:10.1016/j.jsps.2016.12.008
39. Abd El-Rehim HA, El-Sawy NM, Hegazy ESA, Soliman ESA, Elbarbary AM. Improvement of antioxidant activity of chitosan by chemical treatment and ionizing radiation. *Int J Biol Macromol*. 2012;50(2):403-413. doi:10.1016/j.ijbiomac.2011.12.021
40. Vieira ACC, Chaves LL, Pinheiro S, et al. Mucoadhesive chitosan-coated solid lipid nanoparticles for better management of tuberculosis. *Int J Pharm*. 2018;536(1):478-485. doi:10.1016/j.ijpharm.2017.11.071
41. García MA, Pinotti A, Martino MN, Zaritzky NE. Characterization of composite hydrocolloid films. *Carbohydr Polym*. 2004;56:339-345. doi:10.1016/j.carbpol.2004.03.003
42. Kwok DY, Neumann AW. Contact angle measurement and contact angle interpretation. *Adv Colloid Interface Sci*. 1999;81(3):167-249. doi:10.1016/S0001-8686(98)00087-6
43. Usta SN, Solana C, Ruiz-Linares M, et al. Effectiveness of conservative instrumentation in root canal disinfection. *Clin Oral Investig*. 2023;1:1-8. doi:10.1007/S00784-023-04929-Z/TABLES/2
44. Farrugia C, Lung CYK, Schembri Wismayer P, Arias-Moliz MT, Camilleri J. The relationship of surface characteristics and antimicrobial performance of pulp capping materials. *J Endod*. 2018;44(7):1115-1120. doi:10.1016/j.joen.2018.04.002
45. de Chávez Paz LE. Image analysis software based on color segmentation for characterization of viability and physiological activity of biofilms. *Appl Environ Microbiol*. 2009;75(6):1734-1739. doi:10.1128/AEM.02000-08
46. Singh R, Lillard JW. Nanoparticle-based targeted drug delivery. *Exp Mol Pathol*. 2009;86(3):215-223. doi:10.1016/j.yexmp.2008.12.004
47. Pawar V, Topkar H, Srivastava R. Chitosan nanoparticles and povidone iodine containing alginate gel for prevention and treatment of orthopedic implant associated infections. *Int J Biol Macromol*. 2018;115:1131-1141. doi:10.1016/j.ijbiomac.2018.04.166
48. Ing LY, Zin NM, Sarwar A, Katas H. Antifungal activity of chitosan nanoparticles and correlation with their physical properties. *Int J Biomater*. 2012;26:1-9. doi:10.1155/2012/632698
49. Azizian S, Hadjizadeh A, Niknejad H. Chitosan-gelatin porous scaffold incorporated with chitosan nanoparticles for growth factor delivery in tissue engineering. *Carbohydr Polym*. 2018;202:315-322. doi:10.1016/j.carbpol.2018.07.023
50. Song F, Koo H, Ren D. Effects of material properties on bacterial adhesion and biofilm formation. *J Dent Res*. 2015;94(8):1027-1034. doi:10.1177/0022034515587690
51. Camilleri J, Arias Moliz T, Bettencourt A, et al. Standardization of antimicrobial testing of dental devices. *Dent Mater*. 2020;36(3):e59-e73. doi:10.1016/j.dental.2019.12.006
52. Boutsoukios C, Arias-Moliz MT, Chávez de Paz LE. A critical analysis of research methods and experimental models to study irrigants and irrigation systems. *Int Endod J*. 2022;55(5):295-329. doi:10.1111/IEJ.13710
53. Ruiz-Linares M, Solana C, Baca P, Arias-Moliz MT, Ferrer-Luque CM. Antibiofilm potential over time of a tricalcium silicate material and its association with sodium diclofenac. *Clin Oral Investig*. 2022;26(3):2661-2669. doi:10.1007/S00784-021-04237-4/FIGURES/2
54. Helander IM, Nurmiäho-Lassila EL, Ahvenainen R, Rhoades J, Roller S. Chitosan disrupts the barrier properties of the outer membrane of gram-negative bacteria. *Int J Food Microbiol*. 2001;71(2-3):235-244. doi:10.1016/S0168-1605(01)00609-2
55. Khan F, Pham DTN, Oloketuyi SF, Manivasagan P, Oh J, Kim YM. Chitosan and their derivatives: Antibiofilm drugs against pathogenic bacteria. *Colloids Surf B Biointerfaces*. 2020;185:110627. doi:10.1016/J.COLSURFB.2019.110627
56. Abdelgawad AM, Hudson SM, Rojas OJ. Antimicrobial wound dressing nanofiber mats from multicomponent (chitosan/silver-NPs/polyvinyl alcohol) systems. *Carbohydr Polym*. 2014;100:166-178. doi:10.1016/j.carbpol.2012.12.043
57. Misra R, Sahoo SK. Antibacterial activity of doxycycline-loaded nanoparticles. *Methods Enzymol*. 2012;509:61-85. doi:10.1016/B978-0-12-391858-1.00004-6
58. Mohamed MA, Nasr M, Elkhatib WF, Eltayeb WN, Elshamy AA, El-Sayyad GS. Nanobiotic formulations as promising advances for combating MRSA resistance: susceptibilities and post-antibiotic effects of clindamycin, doxycycline, and linezolid. *RSC Adv*. 2021;11(63):39696-39706. doi:10.1039/D1RA08639A
59. Cerchiara T, Abruzzo A, Nahui Palomino RA, et al. Spanish broom (*Spartium junceum* L.) fibers impregnated with vancomycin-loaded chitosan nanoparticles as new antibacterial wound dressing: preparation, characterization and antibacterial activity. *Eur J Pharm Sci*. 2017;99:105-112. doi:10.1016/j.ejps.2016.11.028
60. Vardanyan RS, Hruby VJ. Antibiotics. *Synth Essent Drugs*. 2006;1:425-498. doi:10.1016/B978-044452166-8/50032-7
61. Sanz R, Calpena AC, Mallandrich M, Gimeno Á, Halbaut L, Clares B. Development of a buccal doxepin platform for pain in oral mucositis derived from head and neck cancer treatment. *Eur J Pharm Biopharm*. 2017;117:203-211. doi:10.1016/J.EJPB.2017.04.019
62. Macedo D, Filho AJMC, Soares de Sousa CN, et al. Antidepressants, antimicrobials or both? Gut microbiota dysbiosis in depression and possible implications of the antimicrobial effects of antidepressant drugs for antidepressant effectiveness. *J Affect Disord*. 2017;208:22-32. doi:10.1016/J.JAD.2016.09.012
63. Caldara M, Marmioli N. Tricyclic antidepressants inhibit *Candida albicans* growth and biofilm formation. *Int J Antimicrob Agents*. 2018;52(4):500-505. doi:10.1016/J.IJANTIMICAG.2018.06.023
64. Munoz-Bellido JL, Munoz-Criado S, Garcia-Rodríguez JA. Antimicrobial activity of psychotropic drugs. Selective serotonin reuptake inhibitors. *Int J Antimicrob Agents*. 2000;14(3):177-180. doi:10.1016/S0924-8579(99)00154-5
65. Gillman PK. Tricyclic antidepressant pharmacology and therapeutic drug interactions updated. *Br J Pharmacol*. 2007;151(6):737-748. doi:10.1038/SJ.BJP.0707253
66. Schneider J, Patterson M, Jimenez XF. Beyond depression: other uses for tricyclic antidepressants. *Cleve Clin J Med*. 2019;86(12):807-814. doi:10.3949/CCJM.86A.19005
67. Mandal A, Sinha C, Jena AK, Ghosh S, Samanta A. An investigation on in vitro and in vivo antimicrobial properties of the antidepressant: amitriptyline hydrochloride. *Brazilian J Microbiol*. 2010;41(3):635-642. doi:10.1590/S1517-83822010000300014

## SUPPORTING INFORMATION

Additional supporting information can be found online in the Supporting Information section at the end of this article.

**How to cite this article:** Carrasco Ávila PY, Arias Moliz T, Rosales Leal JI, Baca P, Rodríguez Valverde MÁ, Morales Hernández ME. Novel Ti surface coated with PVA hydrogel and chitosan nanoparticles with antibacterial drug release: An experimental in vitro study. *Clin Implant Dent Relat Res*. 2024;26(2):427-441. doi:10.1111/cid.13305